

Cluster Compounds

[Sn₈]⁶⁻-Bridged Mixed-Valence Zn^I/Zn^{II} in {[K₂ZnSn₈(ZnMes)]₂}⁴⁻ Inverse Sandwich-Type Cluster Supported by a Zn^I-Zn^I Bond

Hong-Lei Xu, Nikolay V. Tkachenko, Alvaro Muñoz-Castro, Alexander I. Boldyrev,* and Zhong-Ming Sun*

Abstract: Since [Sn₈]⁶⁻ was discovered from the solid-state phase in 2000, its solution chemistry has been elusive due to the high charges and chemical activity. Herein, we report the synthesis and characterization of an inverse sandwich-type cluster dimer {[K₂ZnSn₈(ZnMes)]₂}⁴⁻ (**1a**), in which the highly charged [Sn₈]⁶⁻ is captured by mixed-valence Zn^I/Zn^{II} to form the dimer {closo-[Zn₂Sn₈]₂} moieties bridged by a Zn-Zn bond. Such Zn-Sn cluster not only exhibits a novel example of mixed-valence Zn^I/Zn^{II} for stabilizing highly active anion species, but also indicates the [Sn₈]⁶⁻ cluster can act as a novel bridging ligand, like arene, with a η^4 : η^4 -fashion. Theoretical calculations indicate that a significant delocalization of electrons over Zn atoms plays a vital role in the stabilization of the [Sn₈]⁶⁻ species. The AdNDP and magnetic response analyses clearly showed the presence of local σ -aromaticity in three cluster fragments: two ZnSn₄ caps and Sn₈ square antiprism.

Polyhedral boranes have been attracting great interest due to their extraordinary performances in all branches of chemistry.^[1] Fascinating structures brought the pathbreaking bonding patterns. The situation induced the development of Wade rules, which helped us figure out the relationship between geometric structures of borane clusters and their electronic structures.^[2] For example, deltahedral closo-boranes [B_nH_n]²⁻ obey the electron counting rules of borane structures, that they should possess $n+1$ electron pairs where n is the number of vertices. As in the case of a polyhedron with missing vertices, namely *nido* or *arachno*, the number of skeletal electron pairs needs to satisfy $n+1+p$ (p is the number of missing vertices) for the stability of skeletons. As the isoelectronic relationship between fragments {BH} and E atoms (E = Si–Pb), these rules have been long borrowed to

How to cite:

International Edition: doi.org/10.1002/anie.202102578

German Edition: doi.org/10.1002/ange.202102578

illustrate and predict the related structures from group 14.^[3] Expectedly, the *closo*-[E₅]²⁻ (E = Si, Ge, Sn, Pb) and [E₁₀]²⁻ (E = Ge, Pb) as an isostructural and isoelectronic species with corresponding boranes [B₅H₅]²⁻ and [B₁₀H₁₀]²⁻ have been isolated from solutions,^[4] whereas the very stable *closo*-structures limit their reactivity in solutions.^[5] In contrast, the *nido*-clusters of [E₉]⁴⁻ (E = Si, Ge, Sn, Pb) and [E₄]⁴⁻ (E = Si, Ge, Sn) have exhibited good reactivity and accounted for a number of new derivatives,^[6] such as oxidative coupling,^[7] functionalization with main-group/transition-metal fragments,^[8–11] cluster fusion and assembly.^[12] Hence, it is foreseeable that the solution chemistry of [E₈]⁶⁻ clusters of missing two vertices from the [E₁₀]²⁻ will be fascinating. The observation of [Sn₈]⁶⁻ in solid-state Zintl phases A₄Li₂Sn₈ (A = K, Rb) and Ba₁₆Na₂₀₄Sn₃₁₀^[13] shows the existence of such species as predicted by Wade's rules. However, it still remains challenging to bring the cluster into solution^[14] and thus related derivative has been elusive so far. Herein, we report a new cluster anion {[K₂ZnSn₈(ZnMes)]₂}⁴⁻ (**1a**) as a [K(2,2,2-crypt)]⁺ salt (**1**) containing two individual Sn₈ units stabilized by two groups of capped Zn atoms and combined with a Zn-Zn bond. The successful preparation of **1** not only represents a rare example of the mixed-valence Zn^I/Zn^{II} together for capturing highly charged anion species, but might open the way to solution chemistry of multiple vertex deficient main-group metal clusters. The title compound, [K(2,2,2-crypt)]₄·{[K₂ZnSn₈(ZnMes)]₂} (**1**), was synthesized by solution reaction of "K₄ZnSn₄" and ZnMes₂ in the presence of 2,2,2-crypt. After 20 days, dark-red plate crystals were observed in the test tube (21% yield based on loaded starting material ZnMes₂, see supporting information). The X-ray diffraction analysis (XRD) reveals that the compound crystallizes in the monoclinic space group P2₁/n and there is one cluster anion {[K₂ZnSn₈(ZnMes)]₂}⁴⁻ (**1a**) with four [K(2,2,2-crypt)]⁺ counter cations in the molecular structure. (Figure S3). Additional characterization of energy-dispersive X-ray spectroscopy (EDS, Figure S10) showed the composition of **1** including K, Zn, and Sn elements. Electrospray-ionization mass spectrometry (ESI-MS) and ¹¹⁹Sn NMR spectroscopy were also attempted, but the related characterizations suffered from failure due to inevitable fast decomposition of **1** in DMF solutions.

At first glance, the cluster anion **1a** exhibits a specific dimeric structure containing two identical subunits of [ZnSn₈(ZnMes)] which are surrounded by four non-cryptated K-cations (Figure 1a,b). The four free K-cations around the neck of the whole cluster construct a square plane with K-K distances ranging from 4.762 to 4.878 Å. Although the long distances between four surrounding K-cations and Sn atoms

[*] H.-L. Xu, Prof. Dr. Z.-M. Sun

State Key Laboratory of Elemento-Organic Chemistry, Tianjin Key Lab for Rare Earth Materials and Applications, School of Materials Science and Engineering, Nankai University
Tianjin 300350 (China)
E-mail: sunlab@nankai.edu.cn

N. V. Tkachenko, Prof. Dr. A. I. Boldyrev
Department of Chemistry and Biochemistry, Utah State University
0300 Old Main Hill, Logan, UT 84322-0300 (USA)
E-mail: a.i.boldyrev@usu.edu

Prof. Dr. A. Muñoz-Castro
Grupo de Química Inorgánica y Materiales Moleculares, Facultad de Ingeniería, Universidad Autónoma de Chile
El Llano Subercaseaux, Santiago 2801 (Chile)

Supporting information and the ORCID identification number(s) for the author(s) of this article can be found under <https://doi.org/10.1002/anie.202102578>.

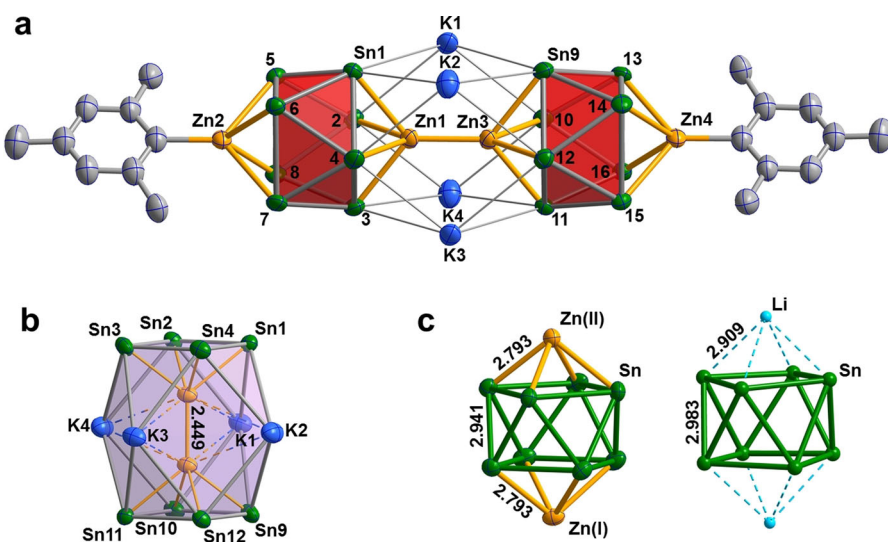


Figure 1. a) ORTEP representation of the cluster anion $\{[K_2ZnSn_8(ZnMes)]_2\}^{4-}$ (thermal ellipsoids are drawn at 50% probability). b) The structure of fragment $[K_4Zn_2Sn_8]$ is shown by a rotation of 90 degrees. The Zn-Zn bond length is given in Å. c) The contrast of *closo*- $[Zn_2Sn_8]$ moiety in anion **1a** and *closo*- $[\text{Li}_2Sn_8]^{4-}$ in the Zintl phase $K_4\text{Li}_2Sn_8$.^[13a] The average bond lengths are given in Å.

(K-Sn: $3.775(3)$ – $3.837(4)$ Å) indicate weak interactions, the K-cations play a vital role in the formation and stabilization of the unusual highly charged dimeric product based on the fact that crystals of **1** cannot be isolated by adding the excess of 2,2,2-crypt under parallel experiments. The K-cations act as an attractive force to pull the two anions together by screening their charges and thus allowing them to dimerize. Such situation is also observed in $[\text{Ge}_9\text{Ge}_9]^{6-}$ and $[\text{Ge}_9\text{Zn-ZnGe}_9]^{6-}$.^[7a,15] Additionally, **1a** can also be viewed as a sandwich-type structure where a dinuclear $[\text{Zn-Zn}]^{2+}$ unit is flanked by two heteroatomic cluster anions of $[\text{Sn}_8\text{ZnMes}]^{5-}$. However, it should be better described as a multilayer inverse-sandwich dimer in which both $[\text{Sn}_8]^{6-}$ units are respectively jammed by $[\text{Zn}^{\text{II}}\text{Mes}]$ and Zn^{I} and then combined with a Zn-Zn bond, thus the structure is supported by four surrounding K- cations. According to Wade-Mingos rules,^[2] the cluster bonding electrons would be 22 for a ten-vertex *closo*-species. In this sense, the $[\text{Sn}_8]^{6-}$ capped by two Zn atoms forms a heteroatomic *closo*-cluster of $[\text{Sn}_8\text{Zn}_2]$ ($6e^- + 8 \times (2e^-) = 22e^-$), with $6e^-$ from the charges, $2e^-$ from each Sn atom and none from the Zn atoms. Hence, on top of the Zn atom is functionalized with -Mes to result in $[\text{ZnSn}_8(\text{ZnMes})]$ with $4e^-$, which is dimerized to form $\{[K_2ZnSn_8(ZnMes)]_2\}^{4-}$.

Zn atoms cap the open square faces of Sn_8 , resulting in the retention of an intact “arachno” structure. Hence, the Sn_8 units in **1a** possess a nearly perfect square antiprism structure (D_{4d}) with two almost parallel bases (Figure 1c). The dihedral angle between the two bases is only 0.33° , similar to that in $[\text{Li}_2\text{Sn}_8]^{4-}$ (0.27° and 0.48°).^[13a] The Sn-Sn bond lengths in the waist ($2.9263(12)$ – $2.9507(12)$ Å) are slightly shorter than those in the bases ($3.1039(10)$ – $3.1615(11)$ Å) and all values ($2.9263(12)$ – $3.1615(11)$ Å) are in the normal range, comparable to those in $[\text{Li}_2\text{Sn}_8]^{4-}$ from $\text{Rb}_4\text{Li}_2\text{Sn}_8$ ($2.947(3)$ – $3.037(2)$ Å), $[\text{Sn}_8\text{TiCp}]^{3-}$ ($2.859(2)$ – $3.108(2)$ Å)^[16] and other Sn clusters, such as $[\text{Sn}_9]^{4-}$ and its derivatives.^[8c,9a,c,12b,17] The distances from the bases of Sn_8 units to their capped Zn atoms

are in a very narrow range of 2.7768 – (18) – $2.8014(18)$ Å, comparing well with those of $2.7397(4)$ – $2.7867(4)$ Å in $[\text{Sn}_9\text{ZnPh}]^{3-}$,^[9c] and this indicates different valences of Zn almost have no effect on the corresponding Zn-Sn bond lengths in **1a**. The Zn-Zn bond acts as a linker between the two $[\text{Sn}_8\text{ZnMes}]$ moieties. Despite the rather high electrostatic repulsion within the highly charged anion $\{[\text{ZnSn}_8(\text{ZnMes})]\}_2^{8-}$, the Zn-Zn bond length ($2.449(3)$ Å) is only slightly longer than those in $[\text{Ge}_9\text{Zn-ZnGe}_9]^{6-}$ ($2.420(1)$ Å)^[15] and other monovalent organozinc species ($2.305(3)$ – $2.430(1)$ Å),^[18] but shorter than the Zn-Zn distances ($2.544(3)$ – $2.831(5)$ Å) in $[\text{K}_2\text{Zn}_{20}\text{Bi}_{16}]^{6-}$.^[19]

To understand the chemical bonding and electronic structure of the investigated cluster, we performed density functional theory (DFT) cal-

culations. All DFT calculations were performed using Gaussian 16 software^[20] at PBE0/defTZVP level of theory.^[21] A detailed description of quantum chemical calculations could be found in the Supporting Information file. The isolated $\{[K_2ZnSn_8(ZnMes)]_2\}^{4-}$ cluster was proved to be a local minimum exhibiting no imaginary frequencies. The optimized structure resembles all essential geometrical features that were found in the experimental X-ray data. The calculated Zn-Zn bond distance is slightly overestimated by 0.1 Å, while the average of Sn-Sn distances is larger by only 0.04 Å. We note that this is a common deviation in calculations of highly charged Zintl anions with DFT methods. The high HOMO-LUMO gap was found for the investigated structure 1.99 eV which is larger than that of $[\text{Sn}_8]^{6-}$ by 0.45 eV, indicating the higher stability of the Zn-containing cluster.

While the role of K-atoms is quite clear in the stabilization of the structure: they provide extra electrons and stabilize the high negative charge of the cluster; the role of Zn atoms is not so obvious. The analysis of molecular orbitals of the $\{[K_2ZnSn_8(ZnMes)]_2\}^{4-}$ shows that Zn participates in the delocalization of electrons via the interaction of vacant $4p$ orbitals of Zn with the linear combinations of Sn $5s/5p$ -orbitals. Thus, the delocalization of electrons over $4p$ Zn-orbitals present in nearly degenerate HOMO, HOMO-1 (Figure S11), and other lower-lying molecular orbitals indicating a significant contribution of Zn in the stabilization of the structure.

Analysis of molecular orbitals provides us a general idea of the role of Zn-atom in cluster stabilization, while electron localization techniques deliver a more illustrative and explicit picture of chemical bonding. To get insight on the localized chemical bonding pattern of $\{[K_2ZnSn_8(ZnMes)]_2\}^{4-}$, we performed an adaptive natural partitioning (AdNDP) analysis of electron density as implemented in AdNDP 2.0 code.^[22] We started the localization procedure from one-center two-electron (1c-2e) elements (lone pairs). We found

that electrons are localized into twenty *d*-type lone pairs on Zn-atom (5 lone pairs per each Zn atom) with occupation numbers (ON) 2.00–1.99 |e| (Figure S12a) and sixteen *s*-type lone pairs on Sn-atom with ON = 1.82–1.79 |e| (Figure S12e). The chemical bonding in organic ligand consists of forty 2c-2e C–C and C–H σ -bonds with ON = 1.99–1.97 |e|. The aromaticity of benzene rings is manifested via six 6c-2e π -bonds with ON = 1.99–1.97 |e| (Figure S12c). The binding between an organic ligand and metal cluster occurs via 2c-2e Zn–C bond with high ON = 1.93 |e|. Two metal clusters are held together by one 2c-2e Zn-Zn σ -bond with ON = 1.85 |e| (Figure S12f). We want to note that although the Zn-Zn distance is quite elongated (presumably due to the electrostatic repulsion), it is a two-center two-electron covalent interaction.

The chemical bonding inside each Zn_2Sn_8 cage can be separated into three structural fragments with delocalized bonding elements: two $ZnSn_4$ caps and Sn_8 square antiprism (Figure 2). We found three 5c-2e σ -bonds per each $ZnSn_4$ cap with ON = 1.98–1.76 |e|. Predictably, we observed a significant contribution of Zn-atoms into those delocalized ele-

ments (29–14 %). The high contribution of Zn-atom confirms that this delocalization plays a crucial role in the stabilization of the investigated cluster. The remaining 20 electrons can be localized into ten 8c-2e σ -bonds (5 bonds per Sn_8 cage) with high ONs = 2.00–1.88 |e|. We note that such delocalization is common in various Zintl clusters.^[23] Remarkably, the presented chemical bonding pattern of the Zn_2Sn_8 cage resembles the chemical bonding in $[Sn_8]^{6-}$ cluster (Figure S13), indicating that Zinc atoms act as a stabilizing factor without significantly changing the chemical bonding pattern in the $[Sn_8]^{6-}$ fragment. It has been discussed before, that the PBE0 functional could overestimate electron delocalization and aromaticity.^[24] To make sure that the obtained results are not a consequence of the choice of the functional, we performed the same calculations using CAM-B3LYP functional^[25] that does not suffer from delocalization error. The obtained results are presented in the SI file (Figure S15) and reproduce results obtained with PBE0 functional.

We note that such delocalization inside each Zn_2Sn_8 cage is usually accompanied by unique magnetic properties, which resembles the behavior of aromatic species.^[12m] The magnetic

criteria of aromaticity^[26] are evaluated to confirm the aromatic behavior of the investigated cluster. The induced magnetic field (B^{ind}), which was evaluated globally along the molecular backbone, contributes to the characterization of aromatic species based on the potential ability to sustain a long-range shielding cone. This behavior is a distinctive feature of both planar and spherically aromatic compounds.^[27] The B^{ind} is related to the applied field (B^{ext}), in terms of the shielding tensor (σ_{ij}) according to the relation $B_i^{ind} = -\sigma_{ii}B_j^{ext}$. Different representative orientations of the B^{ext} are considered via different *i* and *j* suffixes which represent *x*-, *y*- and *z*-axes. The orientationally-averaged term ($(B_{iso})^{ind} = -(1/3)(\sigma_{xx} + \sigma_{yy} + \sigma_{zz})B_j^{ext}$) accounts for the in-solution molecular tumbling.

For orientationally-averaged term, we found a shielding surface originated from each aromatic motif given by mesityl and Zn_2Sn_8 cage fragments, as observed from the contour-plot representation (Figure 3). Under specific orientation of the applied field, the inherent characteristics of the B^{ind} along the series can be depicted. Under *z*-axis orientation, B^{ind} results in a long-range shielding response, with a complementary perpendicular deshielding region. From the contour-plot, it is observed that the overall shielding cone is enabled by the four independent shielding cones from each aromatic motif, where both Zn_2Sn_8 cages share shielding regions of ≈ -8.0 ppm, and mesityl- Zn_2Sn_8 of ≈ -3 ppm. These

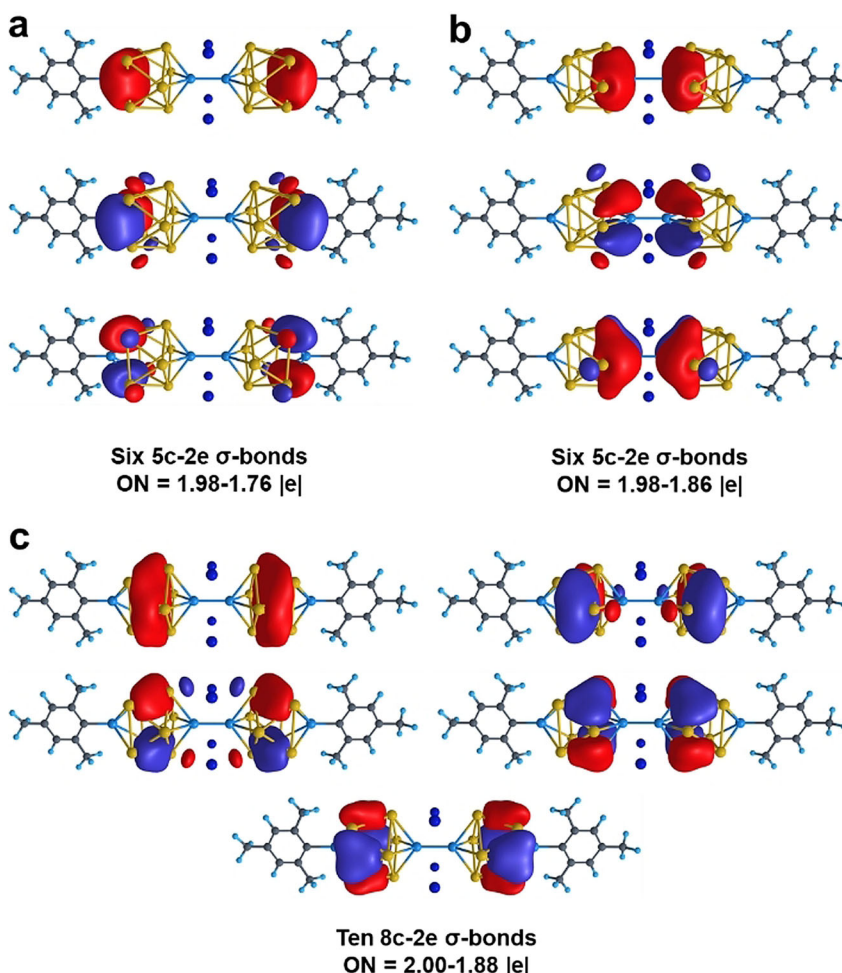


Figure 2. The results of AdNDP analysis for selected delocalized bonding elements of $[K_2ZnSn_8(ZnMes)]_2^{4-}$ cluster. Bonding elements are plotted at an iso-value of 0.03 a.u. Different phases of a wave function represented with different colors. Positive: red; negative: blue. For figure compactness, two multicentered bonds are plotted for each structure.

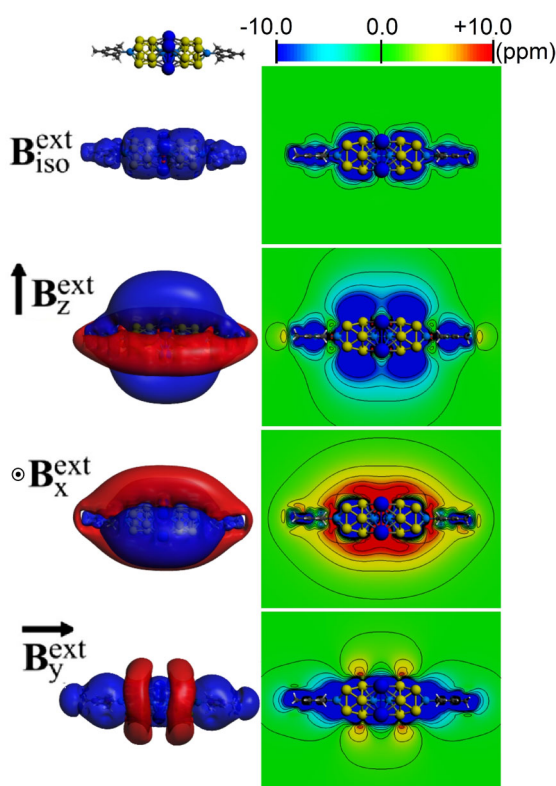


Figure 3. Three-dimensional (left) and contour-plot (right) representation of the magnetic response B^{ind} for $\{[K_2\text{ZnSn}_8(\text{ZnMes})]_2\}^{4-}$. Isosurface values are set at ± 2.0 ppm. Blue: shielding, red, deshielding regions.

results suggest that each aromatic circuit is independent, as denoted by the bonding analysis provided by the AdNDP analysis. Under a field along the x -axis (B_x^{ext}), only Zn_2Sn_8 shielding cones are enabled, denoting the spherical-like aromatic behavior of the ten-membered cage.^[28] Moreover, for a field along the y -axis (B_y^{ext}), two overlapped shielding cones are observed, originated from the spherical-like aromatic characteristic of the bridged Zn_2Sn_8 cages, resulting in an extended shielding region complemented with two deshielding contours centered at each cage.

As a result, we can conclude that the shape of delocalized bonding elements (one bond without a nodal plane, two bonds with one nodal plane, etc.), number of electrons that agrees with Hückel's rule ($6 | e |$ for ZnSn_4 and $10 | e |$ for Sn_8), and peculiar magnetic properties render the described fragments as σ -aromatic. Thus, the chemical bonding inside each Zn_2Sn_8 cage can be described as three locally σ -aromatic fragments: two ZnSn_4 caps and Sn_8 square antiprism.

The analysis of electron localization function (ELF)^[29] confirms the results obtained via AdNDP analysis: we observe the established 2c-2e Zn-Zn bond and a significant delocalization within Zn_2Sn_8 cages (Figure S14a). We also can confirm that there are no K-K or K-Zn covalent interactions (Figure S14b). Thus, K atoms provide the lacking electrons and compensate the overall negative charge of the cluster to stabilize the structure, which also can be confirmed by the highly positive Natural charge of K-atoms (+0.85 a.u.). In

turn, the natural charges of Zn atoms are also positive. Moreover, we can see a clear difference between Zn atoms connected with mesityl ligand and Zn atoms in the Zn_2 fragment. For the former, the calculated natural charge is +1.23 a.u., while for the latter it is +0.60 a.u. The quantum theory of atoms in molecules^[30] and CM5^[31] atomic charge analyses produce qualitatively the same results (Table S3) confirming the formal $\text{Zn}^{\text{I}}/\text{Zn}^{\text{II}}$ oxidation state assignment.

In summary, we have realized the synthesis and isolation of an inverse sandwich-type cluster dimer $\{[K_2\text{ZnSn}_8(\text{ZnMes})]_2\}^{4-}$ involving $[\text{Sn}_8]^{6-}$ and mixed-valence $\text{Zn}^{\text{I}}/\text{Zn}^{\text{II}}$. Such Zn-Sn cluster species indicates the $[\text{Sn}_8]^{6-}$ cluster can act as a potential bridging ligand due to its unusual structure and thus might provide an ideal building unit for constructing new types of one-dimensional materials. In turn, the Zn-Zn bonded cluster anion shows a novel example of mixed-valence $\text{Zn}^{\text{I}}/\text{Zn}^{\text{II}}$ together for capturing anion species, which opens the opportunity for new zinc chemistry.

Acknowledgements

This work was supported by the National Natural Science Foundation of China 21971118 to Z.-M.S. and the USA National Science Foundation (grant CHE-1664379) to A.I.B. A.I.B. also acknowledges financial support from the R. Gauth Hansen Professorship fund. The support and resources from the Centre for High Performance Computing at the University of Utah are gratefully acknowledged. A.M.-C. acknowledges financial support from FONDECYT 1180683. We thank Dr. Ning Li at Rigaku (Beijing) Co., Ltd. for his help on the crystal structure refinements.

Conflict of interest

The authors declare no conflict of interest.

Keywords: $[\text{Sn}_8]^{6-}$ · inverse sandwich · local σ -aromaticity · mixed valence $\text{Zn}^{\text{I}}/\text{Zn}^{\text{II}}$ · Zn-Zn bond

- [1] D. J. Eluvathingal, M. B. Musiri, D. P. Pattath, *J. Am. Chem. Soc.* **2001**, *123*, 4313–4323.
- [2] a) K. Wade, *J. Chem. Soc. D* **1971**, *0*, 792–793; b) D. M. P. Mingos, *Acc. Chem. Res.* **1984**, *17*, 311–319; c) R. E. Williams, *Adv. Inorg. Chem. Radiochem.* **1976**, *18*, 67–142; d) K. Wade, *Adv. Inorg. Chem. Radiochem.* **1976**, *18*, 1–66.
- [3] R. J. Wilson, F. Weigend, S. Dehnen, *Angew. Chem. Int. Ed.* **2020**, *59*, 14251–14255; *Angew. Chem.* **2020**, *132*, 14357–14361.
- [4] a) P. A. Edwards, J. D. Corbett, *Inorg. Chem.* **1977**, *16*, 903–907; b) J. Campbell, G. J. Schrobilgen, *Inorg. Chem.* **1997**, *36*, 4078–4081; c) M. Somer, W. Carrillo-Cabrera, E. M. Peters, K. Peters, M. Kaupp, H. G. von Schnerring, *Z. Anorg. Allg. Chem.* **1999**, *625*, 37–42; d) C. Suchentrunk, N. Korber, *New J. Chem.* **2006**, *30*, 1737–1739; e) J. M. Goicoechea, S. C. Sevov, *J. Am. Chem. Soc.* **2004**, *126*, 6860–6861; f) M. M. Bentlochner, C. Fischer, T. Fässler, *Chem. Commun.* **2016**, *52*, 9841–9843; g) A. Speiermann, S. D. Hoffmann, T. F. Fässler, *Angew. Chem. Int. Ed.* **2006**, *45*, 3459–3462; *Angew. Chem.* **2006**, *118*, 3538–3541.

- [5] a) C. Liu, L. J. Li, Q. J. Pan, Z. M. Sun, *Chem. Commun.* **2017**, 53, 6315–6318; b) D. Rios, S. C. Sevov, *Inorg. Chem.* **2010**, 49, 6396–6398.
- [6] a) J. M. Goicoechea, S. C. Sevov, *Organometallics* **2006**, 25, 5678–5692; b) R. J. Wilson, N. Lichtenberger, B. Weinert, S. Dehnen, *Chem. Rev.* **2019**, 119, 8506–8554; c) S. Scharfe, F. Kraus, S. Stegmaier, A. Schier, T. F. Fässler, *Angew. Chem. Int. Ed.* **2011**, 50, 3630–3670; *Angew. Chem.* **2011**, 123, 3712–3754.
- [7] a) L. Xu, S. C. Sevov, *J. Am. Chem. Soc.* **1999**, 121, 9245–9246; b) A. Ugrinov, S. C. Sevov, *J. Am. Chem. Soc.* **2002**, 124, 10990–10991; c) A. Ugrinov, S. C. Sevov, *Inorg. Chem.* **2003**, 42, 5789–5791; d) R. Hauptmann, T. F. Fässler, *Z. Anorg. Allg. Chem.* **2003**, 629, 2266–2273; e) R. Hauptmann, T. F. Fässler, *Z. Anorg. Allg. Chem.* **2004**, 630, 1977–1981; f) L. Yong, S. D. Hoffmann, T. F. Fässler, *Z. Anorg. Allg. Chem.* **2005**, 631, 1149–1153.
- [8] a) A. Ugrinov, S. C. Sevov, *J. Am. Chem. Soc.* **2003**, 125, 14059–14064; b) M. W. Hull, S. C. Sevov, *Angew. Chem. Int. Ed.* **2007**, 46, 6695–6698; *Angew. Chem.* **2007**, 119, 6815–6818; c) D. J. Chapman, S. C. Sevov, *Inorg. Chem.* **2008**, 47, 6009–6013; d) M. W. Hull, S. C. Sevov, *J. Am. Chem. Soc.* **2009**, 131, 9026–9037; e) F. Li, S. C. Sevov, *Inorg. Chem.* **2012**, 51, 2706–2708; f) F. Li, A. Muñoz-Castro, S. C. Sevov, *Angew. Chem. Int. Ed.* **2012**, 51, 8581–8584; *Angew. Chem.* **2012**, 124, 8709–8712; g) M. M. v. Bentlohner, W. Klein, Z. H. Fard, L. A. Jantke, T. F. Fässler, *Angew. Chem. Int. Ed.* **2015**, 54, 3748–3753; *Angew. Chem.* **2015**, 127, 3819–3824; h) F. S. Geitner, W. Klein, T. F. Fässler, *Angew. Chem. Int. Ed.* **2018**, 57, 14509–14513; *Angew. Chem.* **2018**, 130, 14717–14721; i) F. S. Geitner, J. V. Dums, T. F. Fässler, *J. Am. Chem. Soc.* **2017**, 139, 11933–11940; j) C. Wallach, F. S. Geitner, A. J. Karttunen, T. F. Fässler, *Angew. Chem. Int. Ed.* **2021**, 60, 2648–2653; *Angew. Chem.* **2021**, 133, 2680–2685; k) A. Ugrinov, S. C. Sevov, *J. Am. Chem. Soc.* **2002**, 124, 2442–2443; l) F. Li, A. Muñoz-Castro, S. C. Sevov, *Angew. Chem. Int. Ed.* **2016**, 55, 8630–8633; *Angew. Chem.* **2016**, 128, 8772–8775; m) F. Li, S. C. Sevov, *Inorg. Chem.* **2015**, 54, 8121–8125.
- [9] a) B. W. Eichhorn, R. C. Haushalter, *J. Am. Chem. Soc.* **1988**, 110, 8704–8706; b) A. M. Li, Y. Wang, P. Y. Zavalij, F. Chen, A. Muñoz-Castro, B. W. Eichhorn, *Chem. Commun.* **2020**, 56, 10859–10862; c) J. M. Goicoechea, S. C. Sevov, *Organometallics* **2006**, 25, 4530–4536; d) E. N. Esenturk, J. Fettinger, Y. F. Lam, B. W. Eichhorn, *Angew. Chem. Int. Ed.* **2004**, 43, 2132–2134; *Angew. Chem.* **2004**, 116, 2184–2186; e) L. Yong, S. D. Hoffmann, T. F. Fässler, *Eur. J. Inorg. Chem.* **2005**, 3663–3669; f) B. Zhou, M. S. Denning, C. Jones, J. M. Goicoechea, *Dalton Trans.* **2009**, 1571–1578; g) S. Scharfe, T. F. Fässler, *Eur. J. Inorg. Chem.* **2010**, 1207–1213; h) Y. Wang, Q. Qin, J. Y. Wang, R. L. Sang, L. Xu, *Chem. Commun.* **2014**, 50, 4181; i) F. S. Geitner, T. F. Fässler, *Chem. Commun.* **2017**, 53, 12974–12977.
- [10] a) J. M. Goicoechea, S. C. Sevov, *J. Am. Chem. Soc.* **2006**, 128, 4155–4161; b) J. Q. Wang, S. Stegmaier, B. Wahl, T. F. Fässler, *Chem. Eur. J.* **2010**, 16, 1793–1798; c) J. Q. Wang, S. Stegmaier, T. F. Fässler, *Angew. Chem. Int. Ed.* **2009**, 48, 1998–2002; *Angew. Chem.* **2009**, 121, 2032–2036; d) B. Zhou, M. S. Denning, D. L. Kays, J. M. Goicoechea, *J. Am. Chem. Soc.* **2009**, 131, 2802–2803; e) B. Kesani, J. Fettinger, D. R. Gardner, B. Eichhorn, *J. Am. Chem. Soc.* **2002**, 124, 4779–4786.
- [11] a) S. Stegmaier, M. Waibel, A. Henze, L. A. Jantke, A. J. Karttunen, T. F. Fässler, *J. Am. Chem. Soc.* **2012**, 134, 14450–14460; b) M. Waibel, F. Kraus, S. Scharfe, B. Wahl, T. F. Fässler, *Angew. Chem. Int. Ed.* **2010**, 49, 6611–6615; *Angew. Chem.* **2010**, 122, 6761–6765; c) C. B. Benda, M. Waibel, T. Kçchner, T. F. Fässler, *Chem. Eur. J.* **2014**, 20, 16738–16746; d) F. Fendt, C. Koch, S. Gartner, N. Korber, *Dalton Trans.* **2013**, 42, 15548–15550; e) T. Henneberger, W. Klein, J. V. Dums, T. F. Fässler, *Chem. Commun.* **2018**, 54, 12381–12384; f) C. Wallach, K. Mayer, T. Henneberger, W. Klein, T. F. Fässler, *Dalton Trans.* **2020**, 49, 6191–6198; g) M. Waibel, T. Henneberger, L. A. Jantke, T. F. Fässler, *Chem. Commun.* **2012**, 48, 8676–8678.
- [12] a) B. Kesani, J. E. Halsig, P. Zavalij, J. C. Fettinger, Y. F. Lam, B. W. Eichhorn, *J. Am. Chem. Soc.* **2007**, 129, 4567–4574; b) F. S. Geitner, W. Klein, T. F. Fässler, *Dalton Trans.* **2017**, 46, 5796–5800; c) Z. M. Sun, H. Xiao, J. Li, L. S. Wang, *J. Am. Chem. Soc.* **2007**, 129, 9560–9561; d) J. M. Goicoechea, S. C. Sevov, *J. Am. Chem. Soc.* **2005**, 127, 7676–7677; e) J. M. Goicoechea, S. C. Sevov, *Angew. Chem. Int. Ed.* **2005**, 44, 4026–4028; *Angew. Chem.* **2005**, 117, 4094–4096; f) L. G. Perla, S. C. Sevov, *Angew. Chem. Int. Ed.* **2016**, 55, 6721–6724; *Angew. Chem.* **2016**, 128, 6833–6836; g) B. Zhou, M. S. Denning, T. A. D. Chapman, J. E. McGrady, J. M. Goicoechea, *Chem. Commun.* **2009**, 7221–7223; h) C. Liu, X. Jin, L. J. Li, J. Xu, J. E. McGrady, Z. M. Sun, *Chem. Sci.* **2019**, 10, 4394–4401; i) L. G. Perla, S. C. Sevov, *J. Am. Chem. Soc.* **2016**, 138, 9795–9798; j) O. Kysliak, C. Schrenk, A. Schnepf, *Angew. Chem. Int. Ed.* **2016**, 55, 3216–3219; *Angew. Chem.* **2016**, 128, 3270–3274; k) E. N. Esenturk, J. C. Fettinger, B. W. Eichhorn, *J. Am. Chem. Soc.* **2006**, 128, 12–13; l) A. Speckermann, S. D. Hoffmann, F. Kraus, T. F. Fässler, *Angew. Chem. Int. Ed.* **2007**, 46, 1638–1640; *Angew. Chem.* **2007**, 119, 1663–1666; m) H.-L. Xu, I. A. Popov, N. V. Tkachenko, Z.-C. Wang, A. Muñoz-Castro, A. I. Boldyrev, Z.-M. Sun, *Angew. Chem. Int. Ed.* **2020**, 59, 17286–17290; *Angew. Chem.* **2020**, 132, 17439–17443; n) L. G. Perla, A. Muñoz-Castro, S. C. Sevov, *J. Am. Chem. Soc.* **2017**, 139, 15176–15181.
- [13] a) S. Bobev, S. C. Sevov, *Angew. Chem. Int. Ed.* **2000**, 39, 4108–4110; *Angew. Chem.* **2000**, 112, 4274–4276; b) S. Bobev, S. C. Sevov, *J. Am. Chem. Soc.* **2002**, 124, 3359–3365.
- [14] A. Ugrinov, S. C. Sevov, *Appl. Organomet. Chem.* **2003**, 17, 373–376.
- [15] K. Mayer, L. A. Jantke, S. Schulz, T. F. Fässler, *Angew. Chem. Int. Ed.* **2017**, 56, 2350–2355; *Angew. Chem.* **2017**, 129, 2390–2395.
- [16] C. Benda, M. Waibel, T. F. Fässler, *Angew. Chem. Int. Ed.* **2015**, 54, 522–526; *Angew. Chem.* **2015**, 127, 532–536.
- [17] J. D. Corbett, P. Edwards, *J. Chem. Soc. Chem. Commun.* **1975**, 984–985.
- [18] a) I. Resa, E. Carmona, E. Gutierrez-Puebla, A. Monge, *Science* **2004**, 305, 1136–1138; b) T. Li, S. Schulz, P. W. Roesky, *Chem. Soc. Rev.* **2012**, 41, 3759–3771; c) K. Freitag, C. Gemel, P. Jerabek, I. M. Oppel, R. W. Seidel, G. Frenking, H. Banh, K. Dilchert, R. A. Fischer, *Angew. Chem. Int. Ed.* **2015**, 54, 4370–4374; *Angew. Chem.* **2015**, 127, 4445–4449; d) J. Hicks, E. J. Underhill, C. E. Kefalidis, L. Maron, C. Jones, *Angew. Chem. Int. Ed.* **2015**, 54, 10000–10004; *Angew. Chem.* **2015**, 127, 10138–10142.
- [19] A. R. Eulensteiner, Y. J. Franzke, P. Bügel, W. Massa, F. Weigend, S. Dehnen, *Nat. Commun.* **2020**, 11, 5122.
- [20] Gaussian16, RevisionB.01, M. J. Frisch, et al., Gaussian, Inc., Wallingford, **2016**.
- [21] a) A. Schäfer, C. Huber, R. Ahlrichs, *J. Chem. Phys.* **1994**, 100, 5829–5835; b) C. Adamo, V. Barone, *J. Chem. Phys.* **1999**, 110, 6158–6170.
- [22] a) D. Y. Zubarev, A. I. Boldyrev, *Phys. Chem. Chem. Phys.* **2008**, 10, 5207–5217; b) N. V. Tkachenko, A. I. Boldyrev, *Phys. Chem. Chem. Phys.* **2019**, 21, 9590–9596.
- [23] a) N. V. Tkachenko, A. I. Boldyrev, *Chem. Sci.* **2019**, 10, 5761–5765; b) Z.-C. Wang, N. V. Tkachenko, L. Qiao, E. Matito, M. Muñoz-Castro, A. I. Boldyrev, Z.-M. Sun, *Chem. Commun.* **2020**, 56, 6583–6586; c) H.-L. Xu, N. V. Tkachenko, Z.-C. Wang, W.-X. Chen, L. Qiao, A. Muñoz-Castro, A. I. Boldyrev, Z.-M. Sun, *Nat. Commun.* **2020**, 11, 5286.
- [24] C.-R. Irene, R.-C. Eloy, T.-S. Miquel, M. Eduard, *Molecules* **2020**, 25, 711.
- [25] T. Yanai, D. P. Tew, N. C. Handy, *Chem. Phys. Lett.* **2004**, 393, 51–57.

- [26] a) R. Benassi, P. Lazzeretti, F. Taddei, *J. Phys. Chem.* **1975**, *79*, 848–851; b) R. Gershoni-Porannea, A. Stanger, *Chem. Soc. Rev.* **2015**, *44*, 6597–6615.
- [27] a) R. Islas, T. Heine, G. Merino, *Acc. Chem. Res.* **2012**, *45*, 215–228; b) G. Merino, T. Heine, G. Seifert, *Chem. Eur. J.* **2004**, *10*, 4367–4371; c) A. Muñoz-Castro, *Phys. Chem. Chem. Phys.* **2017**, *19*, 12633–12636.
- [28] A. Muñoz-Castro, *ChemPhysChem* **2020**, *21*, 1384–1387.
- [29] a) B. Silvi, A. Savin, *Nature* **1994**, *371*, 683–686; b) T. Lu, F. Chen, *J. Comput. Chem.* **2012**, *33*, 580–592.
- [30] R. F. W. Bader, *Atoms in Molecules: A Quantum Theory*, Clarendon, Oxford, **1990**.
- [31] A. V. Marenich, S. V. Jerome, C. J. Cramer, D. G. Truhlar, *J. Chem. Theory Comput.* **2012**, *8*, 527–541.

Manuscript received: February 20, 2021

Accepted manuscript online: March 7, 2021

Version of record online: ■■■■■

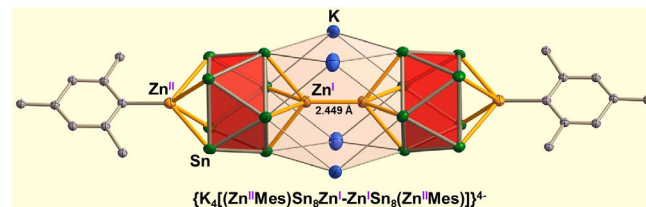
Communications



Cluster Compounds

H.-L. Xu, N. V. Tkachenko,
A. Muñoz-Castro, A. I. Boldyrev,*
Z.-M. Sun*

$[Sn_8]^{6-}$ -Bridged Mixed-Valence Zn^I/Zn^{II} in
 $\{[K_2ZnSn_8(ZnMes)]_2\}^{4-}$ Inverse
 Sandwich-Type Cluster Supported by
 a Zn^I–Zn^I Bond



An inverse sandwich-type cluster dimer of $[K(2,2,2\text{-crypt})]_4\{[K_2ZnSn_8(ZnMes)]_2\}$ was synthesized. The highly charged $[Sn_8]^{6-}$ is captured by mixed-valence Zn^I/Zn^{II} to form the *closo*-[Zn₂Sn₈] bridged by a Zn^I–

Zn^I bond. The Zn–Sn compound not only indicates the $[Sn_8]^{6-}$ can act as a novel bridging ligand like arene, but shows the interdisciplinary integration of cluster chemistry and zinc chemistry.